Daniil, N., Drury, D., & Mellor, P. (2016). Performance comparison of diffusion, circuit-based and kinetic battery models. In 2015 IEEE Energy Conversion Congress and Exposition (ECCE 2015): Proceedings of a meeting held 20-24 September 2015, Montreal, Quebec, Canada. (pp. 1382-1389). (IEEE Energy Conversion Congress and Exposition (ECCE)). Institute of Electrical and Electronics Engineers (IEEE). 10.1109/ECCE.2015.7309854

Performance Comparison of Diffusion, Circuit-based and Kinetic Battery Models

Nikolaos Daniil, David Drury and Phil H. Mellor
Department of Electrical and Electronic Engineering
University of Bristol
Bristol, UK
nikos.daniil@bristol.ac.uk

***Abstract*—Battery models are widely used in the development and operation of battery powered systems. Over the years, a variety of modelling methods have been proposed. In this paper, Circuit-based, Diffusion and Kinetic battery models for a Li-ion polymer battery are compared and the differences on the followed design philosophy are analysed. After the experimental extraction of the parameters, their performance is evaluated. This process is followed in order to choose the most suitable model for a real time application. Thus, apart from accuracy, the execution time in a specific hardware platform is also measured. For the parameterisation and verification of the models, a number of experiments are conducted. The results reveal which model is the best compromise between accuracy and computational effort and indicate the direction of future research to improve the overall performance.**

Keywords—battery modelling; polymer Li-ion; Circuit-based model; Diffusion model; Kinetic battery model; parameter extraction; real time execution; accuracy; power profile

I. INTRODUCTION

Batteries are used in a wide range of applications where an autonomous power supply is required. System designers often consider them to be ideal voltage sources in order to simplify their analysis. This assumption is valid for applications where the battery pack is a secondary system and there is no need for a detailed description. On the contrary, in applications where batteries are a crucial part of the system like Electric Vehicles, deeper analysis of their behaviour is required. Batteries are non-ideal voltage sources and their output depends on the operating conditions and the cycling history. The most important phenomena encountered in battery operation are [1]:

- Open circuit voltage dependence on the remaining charge in the cell.
- Step-down in output voltage when the discharging current is increased. The opposite effect is observed during the charging procedure.
- Usable capacity dependence on the current – Recovery Effect. The total amount of charge delivered by the time the cell voltage drops to cut-off value is lower when the current is high. However, after the discharging process stops, the voltage starts to increase in a recovery process that can last for hours. After the voltage has recovered, the discharging procedure can start again. The opposite effect occurs in charging procedure.
- Coulombic efficiency less than 100%. The maximum amount of charge that a cell can provide is less than the charge required to fully charge it. This phenomenon is often treated as a leakage current during charging [2].
- Voltage and capacity dependence on temperature.
- Self-discharge. A cell being stored for a long time, eventually losses a part of its charge [3].
- Capacity fading. As the battery goes through charging and discharging cycles, the maximum amount of charge that the cell can provide is reduced.

In order to capture the phenomena described above, battery models are widely used. Based on the design philosophy, battery models can be divided in the following categories [4]:

- Electrochemical. These solve the differential equations derived from the chemical reactions and kinetics occurring inside the cell.
- Empirical. These are simple models using intuitive equations or stochastic methods.
- Circuit-based. In this case, an equivalent electrical circuit is used that consists of voltage sources and passive elements. They are widely used because of their ability to run in circuit simulators together with the application circuit.

The scope of this paper is to compare three battery models, highlight the differences in their philosophy and compare their performance. Purpose of this comparison is to select the most suitable model to be used in a real time application. Thus, apart from accuracy the performance criteria will also include ability to run in real time.

The studied models are:

- The Circuit-based model presented in Fig. 1 which is based on [4].

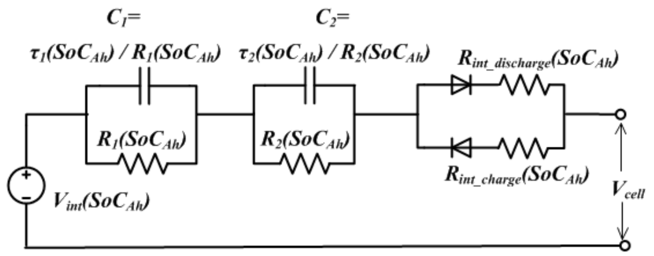

Fig. 1. Circuit-based battery model derived from [4].

- The Diffusion model proposed by Rakhmatov and Vrudhula in [5]. It is a model that lies between Electrochemical and Empirical models. The recovery effect is modelled solving the equation of the diffusion of electroactive species that occurs inside the cell.
- The Kinetic Battery Model (KiBaM) proposed by Manwell and McGowan in [6]. It is a simple empirical model attempting to capture the recovery effect using a hydraulic equivalent system. Initially, it was built for lead-acid batteries but it can be applied in other chemistries as well [7].

A detailed comparison of the last two models is presented in [8] where it is shown that KiBaM can be considered a first order approximation of the Diffusion model. The comparison focuses on their ability to estimate the time-to-discharge, while voltage related effects and overall performance when the cell is being charged are not examined at all. In the end, it is declared that KiBaM is simpler to solve but there is no quantification of this.

In the field of circuit-based models, there is a debate on the number of RC networks that needs to be used. Depending on the application for which the model is developed, the suggested number of RC networks varies. For example in [9], a third RC network is added which has a time constant of hours. On the other hand, [10] compares the accuracy of three circuit models using zero, one and two RC networks and concludes that the best compromise is to use one RC network. However, it should be mentioned that the power profiled used in [10] is based on the driving cycle FTP72 which has short idle times. It is then normal to achieve limited improvement by adding extra RC networks with long time constants. Based on the above, it is decided to use two RC circuits with time constants of seconds and minutes as it is suggested in [4]. A third RC network would increase the complexity and configuration effort with minor benefits in modelling of the dynamic behaviour. On the other hand, using a single RC network would decrease the accuracy when the recovery period is long.

An alternative option to using RC networks in circuit models is presented in [11] where Constant Phase Elements (CPE) replace the capacitors and a Warburg impedance is added in series. The model parameters are extracted in the frequency domain using electrochemical impedance spectroscopy. Reference [12] compares this method (called ZW) with a classic circuit-based model consisting of three RC networks. The comparisons revealed that the ZW method has 5% to 20% higher accuracy but also 1.8 to 4 times higher execution time. Although the improvement in accuracy seems considerable, the reduction of the mean absolute error is always less than 3 mV. Based on these results, it is decided, not to replace RCs with CPEs because this would increase the complexity and configuration effort without any significant improvement in accuracy.

Depending on the application a battery model is used for, the modelling effort could focus on some of the battery characteristics while others could be ignored. This happens in order to simplify the model and shorten the parameterisation procedure. In this paper, the studied models are meant to be used in a real time application. Thus, only the most dynamic characteristics that have an immediate impact on the output voltage will be considered. Such characteristics are voltage dependence on the remaining charge, step voltage change after current changes and recovery effect. Capacity fading and self-discharge are ignored because they are very slow processes that take several days to evolve [3]. Leakage current during charging is also ignored because the studied batteries are of polymer Li-ion chemistry in which the coulombic efficiency is high [13]. Finally, it is assumed that in all the experiments the temperature is constant.

The comparison of the three models is focused on the methods adopted to estimate the open circuit voltage and to capture the recovery effect. All models use an ohmic resistance to justify the instantaneous voltage response in current changes. For increased accuracy, two resistors are used; one for charging and one for discharging operation.

II. Model Philosophy

A. Circuit-based Model

In the Circuit-based model illustrated in Fig. 1, the cell voltage V_{cell} is determined by a circuit consisting of a voltage source, two parallel resistors (one conducts during charging and the other during discharging) and two RC networks. All circuit elements are functions of the remaining charge in the cell which in battery litterature is expressed with the term "State of Charge" (*SoC*). For the Circuit-based model to be implemented, *SoC* is estimated based on Ampere-hour (Ah) counting. Assuming that the Ah-counting starts when the battery is fully charged, the Ah-counting State of Charge is defined as:

$$SoC_{Ah} = \frac{\text{Maximum Charge - Removed Charge}}{\text{Maximum Charge}} \cdot 100\% \qquad (1)$$

In (1), maximum charge is equal to the typical capacity given by the manufacturer which for the tested batteries is 1300 mAh or 4680 C.

The implemented Circuit-based model uses two RC networks to describe the recovery effect instead of focusing on the real mechanism that causes it. The first RC circuit has small time constant to model the first seconds of the recovery while the second captures the slower processes that take several minutes. When there is current flowing from the voltage source to the external circuit, an increasing voltage drop is caused by the RC networks while the capacitors are being charged. Once the current is interrupted, the capacitors start to discharge. As a result, the voltage drop is reduced and eventually reaches zero. At the end of the recovery period, the terminal voltage V_{cell} is equal to the value of the voltage source $V_{int}(SoC_{Ah})$.

B. Diffusion Model

In [5], Rakhmatov and Vrudhula attempt to capture the recovery effect studying the diffusion of electroactive species that is the main mechanism causing it. As illustrated in Fig. 2a and 2b, when the cell is discharged there is consumption of electroactive species close to the electrode surface. This creates a concentration difference between the electrode surface and the main body resulting in diffusion. The diffusion process is generally slower than the rate at which the electroactive species are consumed. The result of this is illustrated in Fig. 2b where the discharging procedure has to stop because the battery seems to be fully discharged. However, there is still some charge remaining in the battery which eventually gets closer to the electrode surface in a recovery procedure that ends in Fig. 2c. The reverse procedure occurs during the charging procedure as it is shown in Fig. 2d and 2e.

Assuming that the open circuit battery voltage is a function of the surface concentration of electroactive species, this mechanism can provide a function to describe the recovery effect. The concentration difference is modelled as a mechanism that generates unavailable charge. Solving Fick's laws for diffusion numerically and assuming that initially the battery is fully charged, the equation proposed to describe the available charge is:

$$\sigma(t)=\alpha-\int_0^t i(\tau)dt-\int_0^t i(\tau)\left[2\sum_{m=1}^{\infty} e^{-\beta^2 m^2 (t-\tau)}\right]d\tau=\alpha-l(t)-u(t) \tag{2}$$

Where:

- α — maximum charge that the battery can supply in C
- $i(\tau)$ — flowing current in A, positive when the cell is being discharged
- β — parameter to be determined with units $sec^{-0.5}$
- $l(t)$ — charge removed from the battery in C
- $u(t)$ — unavailable charge in C

The Diffusion model was initially built to compute the remaining battery lifetime. It was designed only for discharging operation during which the surface concentration is always lower than the bulk and the "available" charge less than the actual charge. On the contrary, during the charging procedure, the surface concentration of electroactive species is higher than the bulk as it is shown in Fig. 2d. In other words, the "available" charge would be more than the real charge of the cell which is counter-intuitive. It is suggested then, to use the term "apparent" charge instead. The apparent State of Charge for the Diffusion model can be defined as:

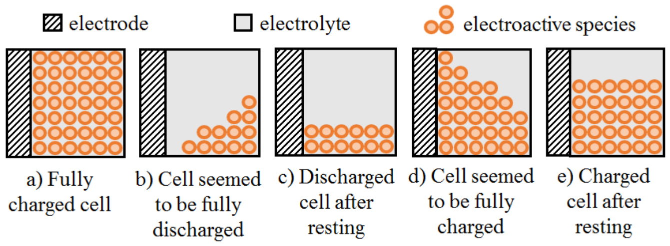

Fig. 2. Diffusion of electroactive species occurring inside the cell as described in [5].

$$SoC_{apparent}(t)=\frac{\text{Initial Charge} - l(t) - u(t)}{\alpha}100\% \tag{3}$$

The final model consists of a voltage source and a series ohmic resistor which are functions of $SoC_{apparent}$. This mechanism is used to capture both the voltage dependency on the remaining charge and the recovery effect.

C. Kinetic Battery Model

KiBaM also treats the recovery effect as a capacity related phenomenon [6]. Similarly to the Diffusion model, a mechanism of available and unavailable charge is proposed to explain the voltage recovery. The difference is that instead of solving the diffusion problem, a hydraulic equivalent system is used to simulate this behaviour. As illustrated in Fig. 3, the battery charge is represented as two tanks separated by a conductance. The first tank contains the charge that is available at any time (available charge). The second tank represents the charge that needs some time to become available either because it is chemically bound or because of the low rate of the diffusion process (bound charge). The battery voltage reaches the cut-off limit when the available charge is depleted. The equations describing the available and the bound charge are:

$$Q_1=Q_{1,0}e^{-kt}+\frac{\left[\left(Q_{1,0}+Q_{2,0}\right)kc-I\right]\left(1-e^{-kt}\right)}{k}-\frac{Ic\left(kt-1+e^{-kt}\right)}{k} \tag{4}$$

$$Q_2=Q_{2,0}e^{-kt}+\left(Q_{1,0}+Q_{2,0}\right)(1-c)\left(1-e^{-kt}\right)-\frac{I(1-c)\left(kt-1+e^{-kt}\right)}{k} \tag{5}$$

The available State of Charge for KiBaM is then defined as:

$$SoC_{available}(t)=\frac{cQ_{max}-Q_1(t)}{Q_{max}}100\% \tag{6}$$

Where:

- Q_1 — available charge in C
- Q_2 — bound charge in C
- I — flowing current in A, positive when the cell is being discharged
- c — width of the available charge well; the bound charge well has width $1-c$
- k — constant indicative for the rate at which the chemically bound charge becomes available
- Q_{max} — maximum total battery charge in C

Similarly to the Diffusion model, the output voltage in KiBaM is estimated by a circuit consisting of a voltage source and a series ohmic resistor which are functions of $SoC_{available}$.

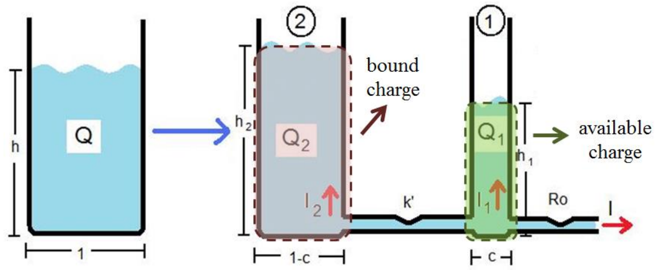

Fig. 3. The hydraulic equivalent mechanism used by Kinetic Battery Model.

III. Experimental Procedure

The battery chosen to be modelled is a 1250-mAh polymer Li-ion VARTA LPP 503562 DL [14] with nominal (or 1C) current 1.25 A. The experiments required to extract the model parameters involve measurements of the battery voltage during charging and discharging cycles with constant and pulsed current. In discharging pulsed current experiments, the cell is discharged with a constant current until it loses 10% of its rated charge (125 mAh) and then it recovers for 1000 sec. After that, the procedure is repeated until the cell reaches the cut-off voltage which is set at 3.2 V. The reverse procedure is followed in charging pulsed current experiments. According to the manufacturer, the battery should be charged with the Constant Current – Constant Voltage (CC-CV) method. For that reason, in all charging experiments, when the voltage reaches the maximum point (set at 4.23 V), the mode is changed to constant voltage. The current values used in parameterisation are 0.2C, 0.5C, 0.8C, 1C and 1.5C (only in discharge). The pulsed current charging and discharging experiments for current 1C are illustrated in Fig. 4. The results of the discharging experiments under constant current are shown in Table I.

Before each discharging experiment, a strict initialization procedure is followed in order to ensure that all the experiments have the same starting point. The battery is fully charged in CC-CV mode. Once the current drops below 0.025 A (0.02C) the process is paused for one hour and then is repeated. One hour after the second charging phase ends, it is assumed that the voltage recovery procedure has practically ended and the battery is ready to undertake an official discharging experiment. A similar procedure is followed before each charging experiment. The cell is discharged with 0.125 A (0.1C) until the voltage drops below the cut-off voltage set at 3.2 V. After an idle period of one hour, this procedure is repeated. One hour after the discharging phase ends for second time, the cell is ready for the official charging experiment.

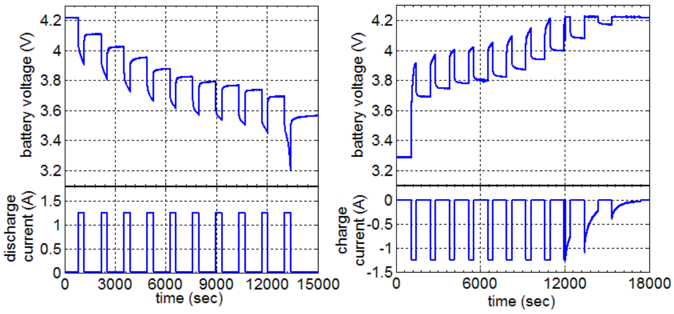

Fig. 4. Discharging and charging experiments with pulsed current used for the parameterization procedures.

TABLE I.

Results of the Constant Current Discharging Experiments

Discharge name	Current (A)	Time to Discharge (sec)	Charge Provided	
			Coulomb	mAh
0.2C	0.250	18562	4640.4	1289
0.5C	0.625	7304	4564.8	1268
1C	1.250	3563	4453.2	1237
1.5C	1.875	2291	4294.8	1193

For all the parameterisation experiments, a half-leg DC-DC converter is used. The control and data acquisition are performed remotely by the dSpace DS1104 R&D Controller Board using a program built in SIMULINK. The time step of the controller is 160 μsec and the data are saved with a 100 msec sampler. During all the experiments, the cell temperature is measured using the built-in NTC of the battery and when necessary, a cooling fan is activated. As a result, the temperature remains at 26 ± 3 °C.

IV. Parameterisation Procedures

A. Circuit-based Model

1) Voltage Source $V_{int}(SoC_{Ah})$: The function describing the voltage source output is derived from voltage measurements at the end of the idle periods in pulsed current experiments. Assuming that idle periods are long enough for the recovery procedure to finish, these values give the value of the voltage source V_{int} for the correspondent Ah-counting State of Charge SoC_{Ah}. Following this procedure in all the experiments, it is observed that for same SoC_{Ah}, the measured V_{int} values for charging cycles are higher than those observed in discharging cycles. This phenomenon is called the hysteresis effect [15]. Modelling of the hysteresis effect is out of the scope of this paper. Hence, a single $V_{int}(SoC_{Ah})$ function is used to smooth this effect. This function is estimated using a 5th order polynomial resulting from curve fitting on voltage measurements from all the pulsed current experiments, as illustrated in Fig. 5.

2) RC networks: These are estimated using voltage measurements in the idle slots of the pulsed experiments. The examined period excludes the immediate voltage changes because they will be modelled by the series resistor. In the idle time between charging pulses, the cell voltage is:

$$V_{cell}(t)=V_{int}+V_{01}exp\left(\frac{-t}{\tau_1}\right)+V_{02}exp\left(\frac{-t}{\tau_2}\right) \qquad (7)$$

Where:

V_{0i} voltage in V of the capacitor C_i when the idle period starts

τ_i time constant in sec of the R_iC_i network

Assuming that the charging current pulse is long enough to fully charge both capacitors, equation (7) becomes:

$$V_{cell}(t)=V_{int}+I_0R_1exp\left(\frac{-t}{\tau_1}\right)+I_0R_2exp\left(\frac{-t}{\tau_2}\right) \qquad (8)$$

$$F(t)=\frac{V_{cell}(t)-V_{int}}{I_0}=R_1exp\left(\frac{-t}{\tau_1}\right)+R_2exp\left(\frac{-t}{\tau_2}\right) \qquad (9)$$

Where:

I_0 amplitude in A of the current pulse which was charging the cell until the beginning of the idle period

The terms τ_1, τ_2, R_1 and R_2 are found by two-term exponential curve fit to function $F(t)$, as it is shown in Fig. 6. The same procedure is followed in the discharging experiments. Using the estimated terms from all the experiments, the parameters of the RC networks are approximated with 3rd or 4th order polynomials as functions of SoC_{Ah}, as illustrated in Fig. 7.

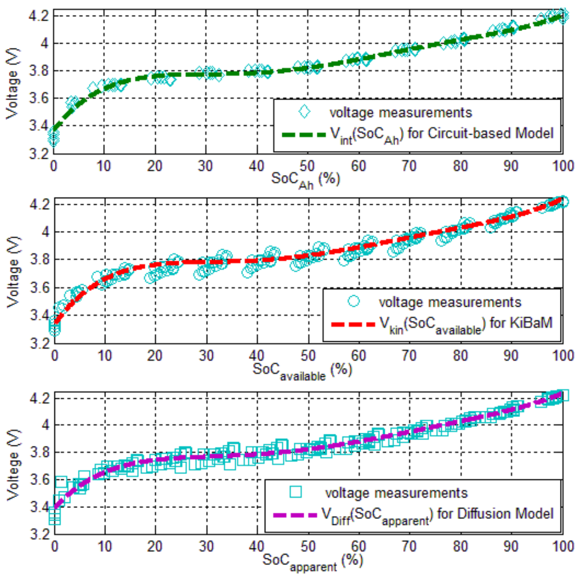

Fig. 5. Curve fitting of the voltage sources used in Circuit-based, Diffusion and Kinetic battery models using 5th order polynomials.

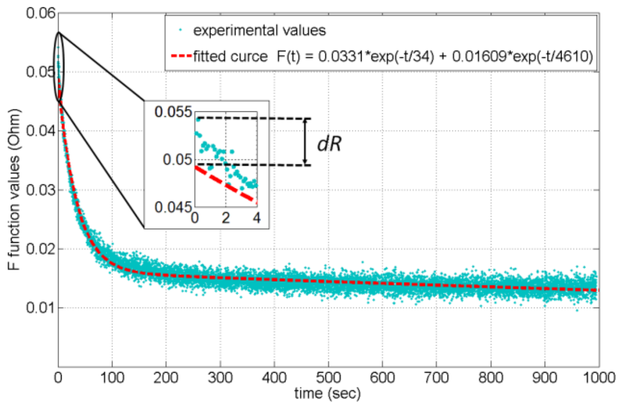

Fig. 6. Curve fitting on the function $F(t)$ shown in (9) which is used to estimate the RC parameters of the Circuit-based battery model. The data points belong to an idle slot of the 1C pulsed current charging experiment but exclude the step voltage change.

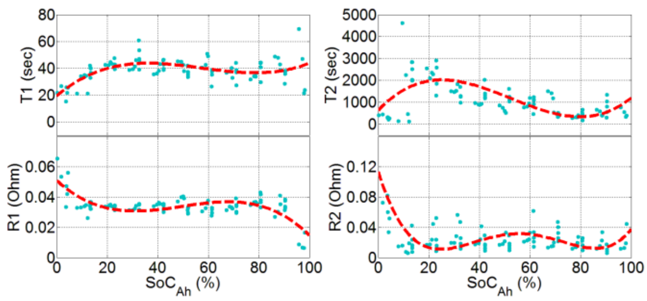

Fig. 7. Estimation of the Circuit-based battery model parameters R_1, R_2, τ_1 and τ_2 as functions of SoC_{Ah} using polynomial curve fitting. The data points are obtained from the process shown in Fig. 6.

a) Simplified Estimation of RC networks: As shown in Fig. 7, the values of R_i and τ_i do not vary significantly with SoC_{Ah}. This is a motive to implement an additional simplified Circuit-based model in which the RC elements will have constant value. It will probably have higher simulation error but also lower execution time.

3) Series Resistor $R_{int}(SoC_{Ah})$: The series ohmic resistor is used to justify the immediate voltage response to changes in current. Thus, it could be calculated using the formula $R=\Delta V/\Delta I$ at the beginning and the end of the current pulses. However, this is not always accurate. As it is illustrated in Fig. 6, the fitting of $F(t)$ can have an initial error dR, which should be added to the estimated resistor value. Using this method for all pulsed current experiments, the series resistor is estimated separately for charging and discharging operation using 5th order polynomials. The fitting of $R_{int}(SoC_{Ah})$ for the discharging cycle is shown in Fig. 8.

B. Diffusion Model

1) Estimation of the parameters α and β: The parameters α and β of the Diffusion model are derived from discharging experiments with constant current using equation (10) [5]:

$$I=\frac{\alpha}{L+2\sum_{m=1}^{10}\frac{1-exp\left(-\beta^2 m^2 L\right)}{\beta^2 m^2}} \tag{10}$$

Table I gives the time-to-discharge L for different values of constant current. After substituting these values in equation (10), the model parameters are estimated using the least square method, as α=4737.8 C and β=0.11578 sec$^{0.5}$.

2) Open Circuit Voltage $V_{Diff}(SoC_{apparent})$: The function relating the open circuit voltage of the Diffusion model V_{Diff} with the apparent State of Charge $SoC_{apparent}$ is found using the discharging pulsed current experiments. The open circuit voltage is measured at the beginning and the end of the idle period and is paired with the correspondent $SoC_{apparent}$ estimated from equation (2). This procedure is illustrated in Fig. 9 for the 1C discharging pulsed current experiment. Following this method for all the pulsed experiments, a set of $SoC_{apparent} - V_{Diff}$ pairs are generated. Those are used as data points to approximate the open circuit voltage for the Diffusion model $V_{Diff}(SoC_{appaerent})$ with a 5th order polynomial as shown in Fig. 5.

3) Series Resistor $R_{Diff}(SoC_{apparent})$: The series resistor is estimated as a function of $SoC_{apparent}$ separately for charging and discharging operation, using Ohm's law $R=\Delta V/\Delta I$ at the beginning and the end of the current pulses. However, relying only on the experimental measurements could reduce the overall model accuracy. An extreme example is illustrated in Fig. 10 where the measured battery voltage and the simulated open circuit voltage $V_{Diff}(SoC_{appaerent})$ for discharging pulsed current operation are plotted.

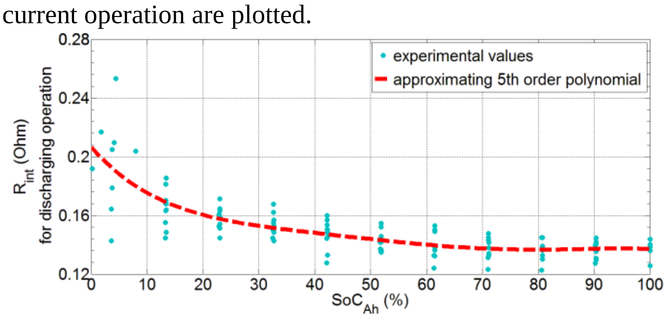

Fig. 8. Approximation of the Circuit-based battery model parameter R_{int} for discharging operation as function of SoC_{Ah} using a 5th order polynomial.

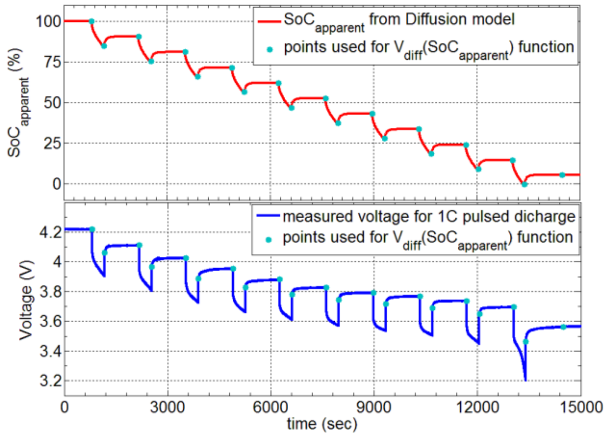

Fig. 9. Battery voltage measurements and the estimated $SoC_{apparent}$ of the Diffusion model during the discharging parameterisation experiment with current pulses of 1C (1.25 A). The highlighted points form the $SoC_{apparent}$ – *Voltage* pairs are used for the polynomial approximation of the Diffusion model open circuit voltage $V_{Diff}(SoC_{apparent})$, as illustrated in Fig. 5.

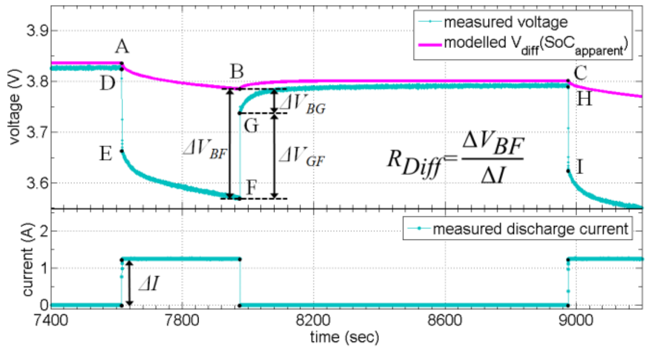

Fig. 10. Battery voltage measurements and simulated open circuit voltage of the Diffusion model $V_{Diff}(SoC_{apparent})$ during a current pulse of 1.25A and the subsequent idle period. The experimental curve is part of the discharging parameterisation experiment with current pulses of 1C.

The simulated BC curve is supposed to model the experimental GH curve during the idle period, but there is a considerable initial error ΔV_{BG}. The value of the series resistor should be selected so that during the current pulse, the simulated AB curve is as close to the experimental EF curve as possible. If ΔV_{GF} is used for the resistance estimation, the error ΔV_{BG} will be transferred. For that reason, ΔV_{BF} is used instead to estimate the model series resistor R_{Diff} value for the specific $SoC_{apparent}$. Following this technique, R_{Diff} is estimated for all the charging and discharging current pulses. These values are used to approximate its value for charging and discharging operation with 5th order polynomials.

C. Kinetic Battery Model

1) Estimation of the parameters k, c and Q_{max}: Parameters for KiBaM are estimated following a procedure similar to the one used for the Diffusion model. The equation relating the parameters c and k with the results of constant current discharging experiments is [6]:

$$\frac{I_1}{I_2} = \frac{[1\text{-}exp(\text{-}kt_2)](1\text{-}c)+kct_2}{[1\text{-}exp(\text{-}kt_1)](1\text{-}c)+kct_1} \tag{11}$$

Where:

I_i discharging current in A

t_i time to discharge in sec under constant current I_i

It is found that the highest simulation accuracy is achieved when applying least squares method with varying I_2 while keeping constant $I_1=1.875\ A$ (1.5C). Thus, the parameters are approximated as $k=0.002945$ and c=0.5988. The maximum charge is estimated $Q_{max}=4697\ C$ using equation (12) [6]:

$$Q_{max} = \frac{It\{[1\text{-}exp(\text{-}kt)](1\text{-}c)+kct\}}{kct} \tag{12}$$

2) Open Circuit Voltage $V_{kin}(SoC_{available})$ and Series Resistor $R_{kin}(SoC_{available})$: In KiBaM, the open circuit voltage and the series resistor for charging and discharging operation are approximated with 5th order polynomials following the same procedure with the Diffusion model. The fitting of the open circuit voltage curve is shown in Fig. 5.

V. Performance Comparison

The three models described in the previous paragraphs and the simplified Circuit-based model with constant RC elements are built in SIMULINK and their performance is tested. The solvers used are ode3 for Diffusion and Circuit-based models and discrete for KiBaM. The results of the overall performance comparison are presented in Table II. The model accuracy is compared using the battery testing power profile PHEV20 [16] and the USABC FUDS test cycle [17] which are illustrated in Fig. 11. Both of them are rated for high power, but for this paper the maximum power is scaled down to 5W. The execution time corresponds to the minimum time step which could be used to run the model (including I/O operations) in real time using a dSpace DS1104 R&D Controller Board with a Power PC MPC 8240 processor at 250MHz.

Table II shows that the Diffusion model has considerably higher execution time than the other models. The reason is that the integral of (2), which is estimated in every step, has to consider all the current values from the beginning of the experiment. A simplified version has been developed which considers only the last 500 sec of the operation and updates the value of the apparent State of Charge $SoC_{apparent}$ in 1-sec steps. This method reduced the execution time from 22000μsec to 450μsec but it is still much longer than the other methods.

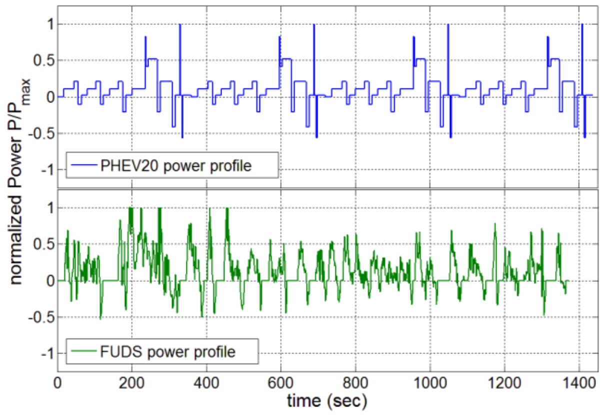

Fig. 11. The power profiles PHEV20 and FUDS used for the model comparison shown in Table II. Positive power indicates discharging operation.

TABLE II.

OVERALL MODEL COMPARISON

Model		configuration effort	execution time step (μsec)	rms error for PHEV20 (mv)	rms error for FUDS (mv)
Circuit-based	variable value of RC	High	25	19	14
	constant value of RC	Medium	22	18	16
	no RC networks used	Very Low	16	26	16
Diffusion		Medium	22000 (450)[a]	21	20
KiBaM		Low	16	20	18

a. The execution time of 450μsec refers to the simplified version of Diffusion Model that updates the apparent charge value in 1sec steps and considers only the last 500sec of the operation.

An additional case that has been tested is a simpler circuit-based model without any RC networks which totally ignores the recovery effect. As shown in Table II, this model has higher simulation error than the other models for the testing profile PHEV20 as expected. On the contrary, in FUDS test cycle the error is relatively small, even smaller than those observed in Diffusion and Kinetic models. This might be counter-intuitive but it can be explained if the two power profiles are compared. In PHEV20, the demanded power remains constant for several seconds during which the recovery effect evolves. In FUDS on the other hand, the power demand changes rapidly. The recovery effect occurring during the discharging slots is partly cancelled by the recovery effect of the subsequent charging slots. As a result, totally ignoring the recovery effect has no considerable effect in model accuracy. This is a special case. In general, simulation accuracy is increased when the recovery effect is considered. Typical examples are shown in Tables III and IV in which the tested power profiles consist of only charging or only discharging pulses.

VI. DISCUSSION

A. Model Selection

The general outcome of Tables II, III and IV is that the highest accuracy is achieved by the Circuit-based model of which the RC elements are functions of the Ah-counting based State of Charge. However, compared to Circuit-based model with constant RC networks, the improvement in accuracy is small. Thus, considering that having varying RC elements increases the complexity and the computational effort, the best compromise is to use RC networks with constant value. KiBaM is the simplest model, but introduces higher errors. High errors are also observed in the Diffusion model which in addition has the disadvantage of high execution time.

B. Sensitivity Analysis

During the processes of parameterisation and model validation, it is important to achieve accurate current measurement. Since the battery experiments are long, even a small current measurement error being integrated for several hours could distort the final results as it is shown in Table V. Another factor that could increase the simulation error is the inaccuracy in estimation of the initial charge in the cell. Table V shows that a small error of 2% (26 mAh) in the initial State of Charge increases the overall simulation error more than 80%.

TABLE III.

SIMULATION ERROR IN 1C PULSED DISCHARGING OPERATION

Experiment at 1.25A		rms error (mV)				
pulse width (mAh)	idle time (sec)	Circuit-based Models: variable value of RC	Circuit-based Models: constant value of RC	Circuit-based Models: no RC	Diffusion Model	KiBaM
250.0	5000	7	7	22	12	12
125.0	1000	7	7	28	20	12
62.5	100	10	11	46	19	17
12.5	10	14	14	51	20	26
constant current		13	13	58	24	41

TABLE IV.

SIMULATION ERROR IN 1C PULSED CHARGING OPERATION (CC-CV METHOD)

Experiment at 1.25A		Rms error (mV)				
pulse width (mAh)	idle time (sec)	Circuit-based Models: variable value of R, C	Circuit-based Models: constant value of R, C	Circuit-based Models: no RC	Diffusion Model	KiBaM
250.0	5000	10	12	27	19	14
125.0	1000	7	10	28	21	14
62.5	100	11	12	42	25	19
12.5	10	14	19	48	24	20
constant current		12	15	47	28	32

TABLE V.

SENSITIVITY ANALYSIS OF THE SIMULATION ERROR FOR CIRCUIT-BASED BATTERY MODEL WITH CONSTANT VALUES OF R AND C

Power Profiles	rms error (mV) with accurate initialisation and current measurements	rms error (mV) with 2% error in the initial SoC	rms error (mV) with current measurement error of: +2%	-2%	+5 mA	-5 mA
FUDS	16	30	26	31	37	38
PVEV20	18	33	31	29	41	36

C. Areas for Improvement in the Circuit-based Model

After concluding that using RC networks is relatively the most suitable method to model the recovery effect, other areas of improvement to be investigated are the voltage source and the series resistor dependence on the remaining charge in the cell. Hence, the performance can be improved in two directions: increasing the accuracy in the State of Charge estimation and achieving lower error in curve fitting procedures.

In all the conducted experiments, the State of Charge estimation error is minimized by following a strict initialisation procedure and accurately calibrating the current. The assumption of 100% coulombic efficiency is valid because Li-ion batteries generally have low leakage current [13]. Since the State of Charge estimation is considered accurate, the alternative field of improvements lies on the curve fitting processes. Concerning the fitted voltage source curve $V_{int}(SoC_{Ah})$, it is very close to the experimental measurements as shown in Fig. 5, where the maximum error is 2%. On the contrary, the differences between the series resistor fitted curve $R_{int}(SoC_{Ah})$ and the measured data points are considerable as seen in Fig. 8. In this case, the maximum error is 25.9%.

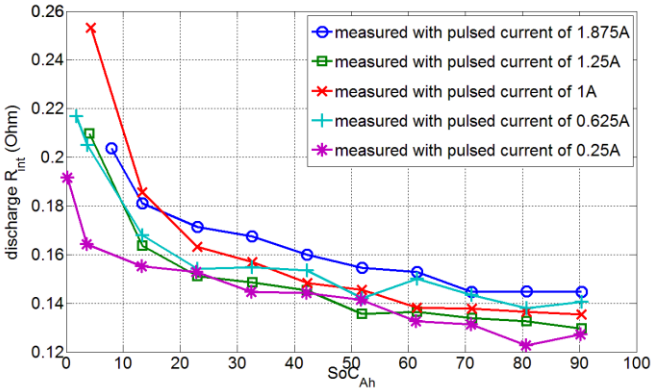

Fig. 12. Values of the Circuit-based model series resistor for discharging operation, as measured in the pulsed current parameterisation experiments.

The error in series resistance curve fitting cannot be attributed to the temperature variations since all the experiments take place at 26 ± 3ºC. Another option considered is to express the series resistor as function of the current. This possibility has been investigated and the results are shown in Fig. 12. There seem to be a trend for increased resistor value when the current is higher but more experiments are required to quantify this. However, working on this direction is not always desirable. A more complex model would increase the configuration effort and the execution time step. Moreover, after a certain number of cycles, ageing effects like capacity fading will emerge that will distort the experimental results [3]. Ignoring the resistor dependence on the current by averaging those curves is a solution frequently encountered in literature which is acceptable in the case that the model is only used during the design and test procedures of a new system. On the other hand, in a real-time application where the battery is physically present (e.g. battery management systems), a model could improve its accuracy by using an observer technique for online correction of the resistor value.

VII. Conclusion

Circuit-based, Diffusion and Kinetic battery models use different techniques to capture the battery recovery effect. The Circuit-based method uses an equivalent circuit representation consisting of RC networks. Diffusion model proposes a method derived from solving the equations that describe the diffusion of electroactive species. KiBaM utilizes an intuitive hydraulic equivalent system separating the total battery charge into "available" and "bound" charge. All three models were parameterized using charging and discharging experiments under constant and pulsed current and they were built in SIMULINK. Subsequently, simulation error and the minimum execution time step for real time operation were compared.

Among them, the Circuit-based model with RC elements estimated as functions of State of Charge has the highest accuracy. However, using constant RC elements is the best compromise because it is easier to configure and has lower execution time without substantially increasing the error. For the power profiles tested, Diffusion and Kinetic battery models showed the lowest accuracy. The power profile selected to test the model accuracy is very important for the comparison outcome. Totally ignoring the recovery effect generally increases the simulation error. However, in the special case where the power profile has rapid changes between charging and discharging cycles, the additional error is small.

A sensitivity analysis for the Circuit-based model has shown that small measurement errors in current or in the initial charge of the cell could result in considerable decrease in simulation accuracy. Apart from this, the most significant factor causing simulation errors is the failure to estimate accurately the value of the series resistor. The solution of considering it to be function of both State of Charge and flowing current has been investigated but rejected because it would increase the implementation complexity.

References

[1] R. Rao, S. Vrudhula, S., D.N. Rakhmatov, "Battery modeling for energy aware system design", *Computer*, vol.36, no.12, pp.77-87, Dec. 2003.

[2] M. Ceraolo, "New dynamical models of lead-acid batteries," *IEEE Transactions on Power Systems* , vol.15, no.4, pp.1184-1190, Nov. 2000.

[3] T.R. Crompton, Battery Reference Book, 3rd edition, McGraw-Hill, 2001.

[4] M. Chen. G.A. Rincon-Mora, "Accurate electrical battery model capable of predicting runtime and I-V performance," *Transactions on Energy Conversion, IEEE*, vol.21, no.2, pp.504-511, June 2006.

[5] D.N. Rakhmatov, S. Vrudhula, "Energy Management for Battery powered Embedded Systems", *ACM Transactions on Embedded Computing Systems*, vol.2:3, pp.277-324, 2003.

[6] J.F. Manwell, J.G. McGowan, "Lead acid battery storage model for hybrid energy systems", *Solar Energy*, vol.50, iss.5, pp.399-405, May 1993.

[7] T. Kim, W. Qiao, "A Hybrid Battery Model Capable of Capturing Dynamic Circuit Characteristics and Nonlinear Capacity Effects," *IEEE Transactions on Energy Conversion*, vol.26, no.4, pp.1172-1180, Dec. 2011.

[8] M.R. Jongerden, B.R. Haverkort, "Which battery model to use?," *IET Software*, vol.3, no.6, pp.445-457, Dec. 2009.

[9] R.C. Kroeze, P.T. Krein, "Electrical battery model for use in dynamic electric vehicle simulations," *IEEE Power Electronics Specialists Conference (PESC 2008)*, 2008, pp.1336-1342.

[10] M. Einhorn, F.V. Conte, C. Kral, J. Fleig, "Comparison, Selection, and Parameterization of Electrical Battery Models for Automotive Applications," *IEEE Transactions on Power Electronics*, vol.28, no.3, pp.1429-1437, March 2013.

[11] S. Buller, M. Thele, R.W. De Doncker, E. Karden, "Impedance-based simulation models of supercapacitors and Li-ion batteries for power electronic applications," *IEEE Transactions on Industry Applications*, vol.41, no.3, pp.742-747, May-June 2005.

[12] D. Andre, M. Meiler, K. Steiner, H. Walz, T. Soczka-Guth, D.U. Sauer, "Characterization of high-power lithium-ion batteries by electrochemical impedance spectroscopy. II: Modelling," *Journal of Power Sources*, vol.196, iss.12, pp.5349-5356, June 2011.

[13] R. Xiong, H. He, F. Sun, K. Zhao, "Evaluation on State of Charge Estimation of Batteries With Adaptive Extended Kalman Filter by Experiment Approach," *IEEE Transactions on Vehicular Technology*, vol.62, no.1, pp.108-117, Jan. 2013.

[14] VARTA, "LPP 503562 DL", 56422201012 datasheet, June 2008.

[15] M.A. Roscher, D.U. Sauer, "Dynamic electric behaviour and open-circuit-voltage modelling of LiFePO4-based lithium ion secondary batteries", *Journal of Power Sources*, vol.196, iss.1, pp.331-336, Jan. 2011.

[16] Idaho National Laboratory, "Battery Test Manual For Plug-In Hybrid Electric Vehicles," Rev. 3, INL/EXT-14-32849, Sep. 2014.

[17] United States Advanced Batteries Consortium, "USABC Electric Vehicle Battery Test Procedure Manual," Rev. 2, U.S. Department of Energy, DOE/ID 10479, January 1996.